^{18}F-FLT PET in Hematologic Disorders: A Novel Technique to Analyze the Bone Marrow Compartment

Ali Agool[1], Bart W. Schot[2], Pieter L. Jager[1], and Edo Vellenga[2]

[1]Department of Nuclear Medicine and Molecular Imaging, University of Groningen and University Medical Center Groningen, Groningen, The Netherlands; and [2]Department of Hematology, University of Groningen and University Medical Center Groningen, Groningen, The Netherlands

Few diagnostic procedures are available to determine the degree of bone marrow cellularity and the numbers of cycling cells in patients with bone marrow disorders. Noninvasive imaging of the bone marrow compartment may be helpful. The PET tracer 3′-fluoro-3′-deoxy-L-thymidine (^{18}F-FLT) has been developed recently. ^{18}F-FLT uptake is related to the rate of DNA synthesis and increases with higher proliferation rates in many types of cancer. Background uptake of ^{18}F-FLT in bone marrow is common. ^{18}F-FLT PET might, therefore, visualize the high cycling activity of hematopoietic cells in the bone marrow compartment. Therefore, we investigated the feasibility of visualization and quantification of the activity of the bone marrow compartment with ^{18}F-FLT PET to distinguish different hematologic disorders. **Methods:** Clinical and laboratory data of 18 patients with myelodysplasia (MDS), chronic myeloproliferative disorders, myelofibrosis, aplastic anemia, or multiple myeloma were correlated with the results of ^{18}F-FLT PET using visual analysis and the standardized uptake value (SUV). Findings were compared with those of healthy control subjects (n = 14). **Results:** With SUV and visual analysis, a distinction could be made between MDS (n = 9), chronic myeloproliferative disorders (n = 3), and myelofibrosis (n = 3) compared with healthy control subjects. A significant increase in ^{18}F-FLT uptake was observed in all of the studied patients with MDS and myeloproliferative disorders. In contrast, patients with myelofibrosis and aplastic anemia (n = 1) demonstrated a decline in bone marrow ^{18}F-FLT uptake compared with healthy control subjects. Comparable results were observed in osteolytic lesions of patients with multiple myeloma (n = 2). **Conclusion:** ^{18}F-FLT PET can be used to visualize the proliferative activity of the bone marrow compartment and may be helpful to distinguish separate hematologic disorders.

Key Words: bone marrow disorders; fluoro-L-thymidine; PET; myelodysplastic syndrome; proliferation

J Nucl Med 2006; 47:1592–1598

In the management of patients with a hematologic disorder, limited diagnostic procedures are available to determine the degree of bone marrow cellularity and the numbers of cycling cells. Primarily a bone marrow biopsy is performed in conjunction with microscopic evaluation. With these methods the bone marrow composition and cellularity can be analyzed. In addition, specific staining procedures can be performed to demonstrate the number of cycling cells. This procedure has distinct limitations: The procedure is invasive and only a very small proportion of the total bone marrow content is investigated, which carries the risk of sampling error. Also, the staining of the bone marrow cells with the monoclonal antibody Ki67, which reflects the number of cycling cells, is an in vitro procedure (*1*). This may not always reflect the in vivo situation.

Noninvasive imaging of the bone marrow cellularity has been pursued using many tracer methods. Bone marrow scintigraphy can be divided into 3 categories based on the 3 target cell systems: red cell precursors, white cell precursors, and tracers for the reticuloendothelial system (RES). For example, in the past, ^{52}Fe was used for imaging of the erythropoietic precursor and ^{59}Fe was used for kinetic studies (*2–4*). The exact target of ^{111}In-chloride, frequently used in the 1970s and 1980s, is unknown (*5,6*). Recently, ^{99m}Tc-labeled antigranulocyte antibodies have been proposed to assess activity of granulocytic cells (*7–9*). Finally, the activity of the RES can be assessed using ^{99m}Tc-labeled colloids. Important problems, however, with all of these agents appear to be nonspecific couptake in the RES (monocytes, macrophages, and so forth), the formation of human antimonoclonal antibodies, or less-desirable imaging properties (^{59}Fe and ^{52}Fe).

The DNA precursor 3′-^{18}F-fluoro-3′-deoxy-L-thymidine (^{18}F-FLT) has been developed recently. Uptake of this tracer is directly related to the rate of DNA synthesis (*10*). Preliminary results with this tracer in several types of cancer patients have demonstrated a high "background" activity in the bone marrow compartment (*11*). This might reflect the high cycling activity of hematopoietic cells in the

Received May 8, 2006; revision accepted Jul. 25, 2006.

For correspondence contact: Pieter L. Jager, MD, PhD, Department of Nuclear Medicine and Molecular Imaging, University Medical Center Groningen, P.O. Box 30,001, 9700 RB Groningen, The Netherlands.

E-mail: p.l.jager@nucl.umcg.nl

bone marrow. However, the exact mechanism of ^{18}F-FLT uptake in bone marrow is still unclear. In several tumor types a relation between ^{18}F-FLT uptake and the proliferation rate has been found, suggesting that the same mechanism could be responsible for the bone marrow uptake (*11*).

The suggested specificity of ^{18}F-FLT uptake for cycling cells, the whole-body imaging aspect, the high resolution of PET, and the quantification possibilities may support the relevance of ^{18}F-FLT PET as a diagnostic procedure in hematologic disorders with bone marrow abnormalities. These aspects could be of great advantage over ^{18}F-FDG PET, which only has a minor uptake in normal bone marrow and might, therefore, be less sensitive. This is the rationale of our study. Patients with myelodysplasia (MDS), chronic myeloproliferative disorders, and myelofibrosis in conjunction with healthy control subjects were studied using the degree of ^{18}F-FLT uptake and the distribution pattern as the main study parameters.

MATERIALS AND METHODS

Patients

Consecutive patients with hematologic disorders were eligible for this study. The precise diagnosis was derived from clinical information and bone marrow biopsies. Patients were divided in 4 groups: MDS, chronic myeloproliferative disorders, myelofibrosis, and a miscellaneous group of patients. Patients with severe renal dysfunction, peripheral neuropathy, or severe elevation of liver enzymes were excluded. All patients provided written informed consent, and the study was approved by the local Medical Ethics Committee of the Groningen University Medical Center.

Control Subjects

Patients with untreated non–small cell lung cancer (NSCLC) or testicular cancer, who had undergone ^{18}F-FLT PET for other studies, were considered as the control subjects. Before inclusion, they were required to have normal blood hematology values and no signs of bone marrow metastases at presentation or during 6 mo of follow-up. In addition, the patients had to be free of chemotherapeutic or radiotherapeutic treatment.

Bone Marrow Examination

Bone marrow biopsy was performed on all patients before ^{18}F-FLT PET, with a maximal interval of 1 mo and a minimal interval of 2 wk. Cellular proliferation was determined in a subgroup using Ki-67 immunostaining with MIB-1 (Ki-67 index) in a selected number of patients (*12*).

^{18}F-FLT PET

^{18}F-FLT was produced according to the method described by Grierson et al. with a radiochemical purity of >95% and a specific activity of >10 TBq/mmol (*13*). Patients were instructed to fast for at least 6 h before investigation, with the exception of free access to water and normal medication. ^{18}F-FLT in a dose of 400 MBq (±10%) was administered intravenously.

Approximately 60 min after the ^{18}F-FLT injection, the patient was placed in the camera, and emission scans of 5 min per bed position and transmission scans of 3 min per bed position were acquired over ~12 bed positions to cover the whole body. An ECAT EXACT HR+ scanner (Siemens Medical Systems) was used for all PET studies. Images were acquired in the 3-dimensional acquisition mode.

Data Analysis

Two nuclear physicians who were unaware of the results of bone marrow biopsy and the clinical diagnosis performed visual and quantitative analysis of ^{18}F-FLT PET images. As this is a new application of ^{18}F-FLT PET, the first readings were independent and a consensus reading was performed afterward. In visual analysis, the overall scan pattern was recorded, and the intensity of bone marrow uptake as well as the degree of bone marrow expansion were evaluated. To quantify bone marrow expansion, we developed a simple scoring system in which 1 point is given for expansion in every one third of the long bones, based on the well-known distribution of ^{18}F-FLT in the central skeleton and ultraproximal part of the femora and humera. Also, the liver and spleen size and the uptake intensity were evaluated qualitatively: + denotes minor uptake intensity, ++ denotes intermediate uptake, and +++ denotes strong uptake intensity.

We also quantified ^{18}F-FLT uptake using standardized uptake value (SUV) analysis in patients and control subjects. We selected several sites of the axial skeleton to sample ^{18}F-FLT activity. These sites were the proximal femur (left and right) at the level of the trochanter major, the iliac crest on both sides, and the corpus of lumbal vertebra 4 and thoracic vertebra 6. In the case of enlargement, the SUV of the liver or spleen was also determined. The region of interests used in SUV analysis were 3-dimensional and were based on the mean value within the 50% isocontour's boundaries using a Siemens Leonardo workstation.

Statistics

For analysis of overall and individual group differences, we used Kruskall–Wallis and Mann–Whitney *U* tests. For correlations, we used Spearman ρ. $P < 0.05$ was considered significant.

RESULTS

Patients

Eighteen patients were included in this study, 10 men (mean age, 69 y) and 8 women (mean age, 64 y). Patient groups included MDS ($n = 9$), according to the International Prognosis Scoring System score belonging to the low-risk or low- to intermediate-risk group (*14*), chronic myeloproliferative disorders ($n = 3$), myelofibrosis ($n = 3$), and a miscellaneous group of patients (aplastic anemia, $n = 1$; multiple myeloma, $n = 2$) (Tables 1 and 2). Fourteen untreated patients with known NSCLC or testis carcinoma were used as the control group. None of the patients had bone marrow involvement and none had undergone chemotherapy or radiotherapy and had normal peripheral blood cell counts.

Visual Analysis and SUV of ^{18}F-FLT PET in Control Subjects

All healthy control subjects were verified to have a qualitatively normal ^{18}F-FLT scan with homogeneous tracer distribution, as known from all previous ^{18}F-FLT studies (Fig. 1) (*15–20*). No bone marrow expansion was observed beyond the axial skeleton, and the size of the liver and spleen was within the normal range. Within the group of healthy control subjects, no difference was observed for

TABLE 1
Patient Characteristics

Patient no.	Diagnosis	Hemoglobulin	Leukocytes	Thrombocytes
Reference value		7.5–9.9 mmol/L	$4-10 \times 10^9$/L	$150-350 \times 10^9$/L
MDS				
1	CMML	7.2	5	161
2	RARS	6.4	8.7	214
3	RA	5.4	1.1	108
4	RA	7.8	4.6	89
5	RA	6.5	6.5	218
6	RA	5.6	9.4	490
7	RARS	5.9	3.2	199
8	RAEB	6.5	10	68
9	RA	5.3	5.9	436
Myeloproliferative disorder				
10		5.7	20.2	244
11		6.5	4.6	404
12		5.2	11.6	170
Myelofibrosis				
13		4.1	1.9	11
14		7.2	7.1	132
15		6.1	16.9	110
Miscellaneous				
16	MM	8.5	4.5	190
17	MM	8.4	4.8	177
18	AA	6.6	1.9	14

CMML = chronic myelomonocytic leukemia; RARS = refractory anemia with ringsideroblasts; RA = refractory anemia; RAEB = refractory anemia with blast excess; MM = multiple myeloma; AA = aplastic anemia.

^{18}F-FLT uptake between the right or left uptake from the same area (Table 3). The lowest uptake was observed in the femura (1.41 ± 0.73) and the highest uptake was in the thoracic and lumbar vertebral body (3.52 ± 1.12 and 3.38 ± 1.05, respectively).

Visual Analysis and SUV in Patient Groups

Overall, significant differences were found between the patient groups for all sites of ^{18}F-FLT uptake (Kruskal–Wallis test; P values between 0.003 and 0.001) and the expansion score ($P < 0.0001$) (Fig. 2).

MDS Group

Visual analysis in 8 MDS patients demonstrated a homogeneous ^{18}F-FLT pattern in the bone marrow (Fig. 3). In 1 patient, ^{18}F-FLT PET showed a patchy uptake with hot spots distributed over the skeleton. SUV analysis of the total MDS group demonstrated significantly increased ^{18}F-FLT uptake in all of the tested bone marrow areas compared with healthy control subjects ($P < 0.001$; Table 3). In addition, a significant expansion of the bone marrow compartment was shown ($P < 0.001$). Liver and splenic uptake was similar to the ^{18}F-FLT uptake in control subjects.

Chronic Myeloproliferative Group

^{18}F-FLT uptake in these 3 patients was homogeneous, with hepatosplenomegaly in 2 (Fig. 4). As expected, this group of patients had remarkable expansion of bone marrow uptake with a mean expansion score of 17.3 ± 8 ($P < 0.0001$ vs. control subjects). This was also higher compared with the MDS group but the difference was not significant. Despite the large size of liver and spleen in 2 patients, ^{18}F-FLT uptake in these organs was not elevated. SUV analysis in this small subgroup yielded higher values than those in the control group in the right femur, both iliac crests, and L4 vertebral body. Values were highest in the L4 and T6 vertebral bodies but no significant difference was observed in comparison with the MDS group. In this patient group, liver and splenic uptake was similar to the uptake in control subjects.

Myelofibrosis Group

^{18}F-FLT uptake was homogeneous in 2 patients but was irregular in 1 patient. Significantly higher uptake in the spleen and liver with distinct hepatosplenomegaly was characteristic of this subgroup compared with healthy control subjects (liver: 3.95 ± 0.11 vs. 2.33 ± 0.74, $P < 0.05$; spleen: 6.0 ± 2.2 vs. 1.46 ± 0.41) (Fig. 5). Bone marrow expansion was also observed, with a mean expansion score of 6.5 ± 5.0. Expansion was significant in 1 patient and moderate in the additional 2 patients. A significant reduced ^{18}F-FLT uptake was found for the left and right crista and for the spine (2.87 ± 0.75 vs. 4.56 ± 1.36, $P < 0.05$).

TABLE 2
^{18}F-FLT Findings in Different Bone Marrow Disorders

Bone marrow disorder	Visual ^{18}F-FLT assessment				SUV ^{18}F-FLT								
	Liver	Spleen	Expansion	General	FemR	FemL	CrR	CrL	L4	T6	Liver	Spine	Spleen
Myelodysplastic disorder													
1	+	+	5	Homogeneous	4.4	4.9	3.3	3.6	5.6	7.1	2.1	7.3	0.8
2	+	−	11	Homogeneous	5.8	5.8	6.8	6.9	8.6	6.6	1.9	8.2	0.9
3	+	+	16	Homogeneous, hepatosplenomegaly	6.8	6.8	7.8	7.6	10.2	9.6	2.1	9.9	2.4
4	++	+	5	Homogeneous, patchy expansion	2.2	1.6	2.4	5.2	9.2	6.9	5.0	8.2	1.3
5	+	+	10	Homogeneous	2.7	2.6	5.3	5.2	5.2	6.6	3.2	6.2	1.5
6	+	−	7	Homogeneous	—	4.6	5.8	5.3	7.1	8.0	2.0	7.8	0.8
7	+	+	2	Homogeneous	8.3	—	5.6	5.7	7.2	7.5	1.9	8.2	1.5
8	+	+	7	Homogeneous	1.8	1.5	4.1	4.3	6.9	8.0	3.8	8.1	0.9
9	+	−	8	Homogeneous	3.0	3.0	4.3	3.9	5.7	6.6	2.2	6.5	1.2
Myeloproliferative disorder													
10	+	+	22	Homogeneous, hepatosplenomegaly	3.8	4.0	3.3	3.2	4.0	3.2	1.2	4.0	1.0
11	+	+	8	Homogeneous	4.0	4.4	5.5	6.8	10.2	8.8	2.4	8.7	1.5
12	+	+	22	Homogeneous, hepatosplenomegaly	5.1	4.9	3.7	3.7	5.0	4.4	1.5	6.0	1.5
Myelofibrosis													
13	+++	+++	20	Inhomogeneous, splenomegaly	1.0	1.0	1.2	1.2	1.8	1.6	4.0	2.0	8.0
14	+++	+++	3	Homogeneous, hepatosplenomegaly	0.9	1.0	1.3	1.4	2.3	3.1	4.0	3.4	6.2
15	+++	+++	10	Homogeneous, hepatosplenomegaly	2.7	2.3	1.4	1.1	3.3	3.3	3.8	3.2	4.0
Miscellaneous													
16	+	+	0	Homogeneous, MM right scapula									
17	+	−	0	Homogeneous, MM crista									
18	+++	+	1	Heterogeneous	0.5	0.5	0.8	1.8	1.7	2.8	4.6	3.1	1.1

FemR = right femur; FemL = left femur; CrR = right crista; CrL = left crista; L4 = lumbar 4 vertebral body; T6 = thoracic 6 vertebral body; MM = multiple myeloma.

Miscellaneous Group

To underscore further that the ^{18}F-FLT uptake is a reflection of the proliferative activity of the bone marrow compartment, 1 patient with aplastic anemia was studied. In addition, osteolytic lesions of 2 multiple myeloma patients were analyzed, as it is known that this malignant plasma cell population has a low proliferative activity. In the patient with aplastic anemia, a strongly reduced ^{18}F-FLT uptake was observed (Table 2). In the multiple myeloma patients, the affected area demonstrated a low ^{18}F-FLT uptake.

Correlations with ^{18}F-FLT Uptake Parameters

In the 10 MDS patients, Ki-67 staining of the bone marrow was available. No correlation was found between ^{18}F-FLT uptake and Ki-67 positivity. For most locations, significant and moderate correlation coefficients (varying between 0.52 and 0.77) between ^{18}F-FLT uptake and the bone marrow expansion scores were found. In addition, a moderate negative correlation of −0.77 was found between the ^{18}F-FLT expansion score and the hemoglobulin level.

DISCUSSION

This feasibility study appears to confirm the value of ^{18}F-FLT PET in various hematologic bone marrow disorders. Compared with control subjects, bone marrow uptake of ^{18}F-FLT was clearly higher in patients with MDS and myeloproliferative disorders but was lower in patients with myelofibrosis, multiple myeloma, and aplastic anemia, in agreement with the cycling activity of the bone marrow compartment of the affected areas. In addition, bone marrow expansion into the peripheral bones was clearly visualized in various degrees in all patients. The combined use of visual analysis and SUV could help distinguish separate hematologic disorders and may be of value for the diagnostic follow-up of this group of patients. In this way, ^{18}F-FLT PET may provide additional information to the data

FIGURE 1. Normal ^{18}F-FLT PET projection image shows uptake in bone marrow in central skeletal compartment limited to ultraproximal extremity bones.

from bone marrow biopsies. ^{18}F-FLT PET, especially, provides a detailed analysis of the entire bone marrow compartment.

In MDS, the increased proliferative activity of erythroid and myeloid cells appears to be followed by an increased programed cell death (*21,22*) and, as a consequence, peripheral pancytopenia. The increased uptake of ^{18}F-FLT in our MDS patients is in agreement with the high proliferative activity of the progenitor cells in the bone marrow compartment (*21*). Although comparable high ^{18}F-FLT SUV values are observed in patients with myeloproliferative disorders, the underlying defects are different. High peripheral blood cell counts are observed frequently in this patient group, which excludes the possibility of increased programed cell death in the bone marrow compartment.

Although ^{18}F-FLT uptake was homogeneous in most patients, there was 1 MDS patient who had a clear patchy ^{18}F-FLT appearance with focal hot spots, possibly indicating "islands" with high bone marrow activity.

In myelofibrosis, the number of cycling bone marrow cells is reduced because of excessive fibrosis, which is in accordance with the low ^{18}F-FLT uptake. In contrast, high SUV values were observed in liver and spleen because of extramedullary hematopoiesis, reflecting proliferative activity of the erythroid and myeloid cells.

The mechanisms governing the uptake of ^{18}F-FLT in bone marrow are not fully clarified. In many tumor types, good correlations between proliferative activity and ^{18}F-FLT uptake have been demonstrated (*11*). Uptake of ^{18}F-FLT appears to be related to the activity of the thymidine kinase-1 enzyme, which is expressed higher in tumor cells, especially during the S-phase of the cell cycle (*23*).

TABLE 3
Mean Uptake Values of ^{18}F-FLT in Various Patient Groups and Healthy Control Subjects

Group	Expansion	FemR	FemL	CrR	CrL	L4	T6	Liver	Spine	Spleen
Control subjects (n = 14)	0	1.41 ± 0.73	1.39 ± 0.68	2.50 ± 0.74	2.50 ± 0.74	3.38 ± 1.05	3.52 ± 1.12	2.33 ± 0.74	4.56 ± 1.36	1.46 ± 0.41
MDS (n = 9)	8.2 ± 4.1*	4.36 ± 2.36*	3.84 ± 1.97*	5.03 ± 1.68*	5.29 ± 1.29*	7.29 ± 1.71*	7.43 ± 1.00*	2.69 ± 1.08	7.81 ± 1.08*	1.27 ± 0.56
Myeloproliferative (n = 3)	17.3 ± 9.2*	4.29 ± 0.69†	4.45 ± 0.46†	4.17 ± 1.21†	4.57 ± 1.91†	6.41 ± 3.35†	5.47 ± 2.94	1.69 ± 0.61	6.22 ± 2.38	1.50 ± 0.03
Myelofibrosis (n = 3)	11 ± 5.0*	1.51 ± 0.98	1.44 ± 0.77	1.32 ± 0.11†	1.23 ± 0.13†	2.44 ± 0.77	2.65 ± 0.91	3.95 ± 0.11†	2.87 ± 0.75†	6.00 ± 2.17*

*$P < 0.001$.
†$P < 0.05$ for comparison with control subjects.
FemR = right femur; FemL = left femur; CrR = right crista; CrL = left crista; T4 = lumbar 4 vertebral body; T6 = thoracic 6 vertebral body.

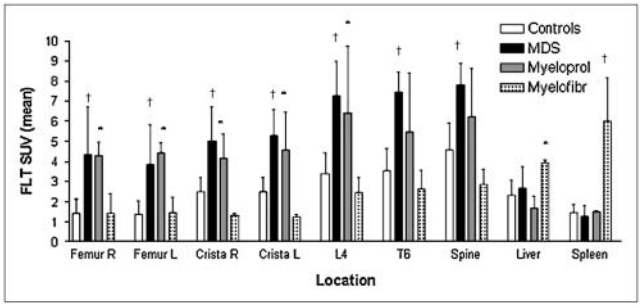

FIGURE 2. Bar graph shows ^{18}F-FLT uptake values (mean SUVs) at various locations. $^{*}P < 0.05$. $^{\dagger}P < 0.001$ for comparison with control subjects. Myeloprol = myeloproliferative disorder; Myelofibr = myelofibrosis.

Presumably the same mechanism accounts for the high uptake in the bone marrow compartment with its high proliferative activity. Uptake of ^{18}F-FLT by the RES is less likely. This assumption is based on previous studies in both patients and laboratory animals, in which only minor uptake of ^{18}F-FLT in inflammatory lesions was observed (*11,24*). However, this assumption needs further validation. No correlation was found with Ki-67 staining. Besides sampling errors, this finding may also be due to the fact that this marker is more suitable to demonstrate a reduced proliferation than an increased proliferation, as normal bone marrow cells already demonstrate high proliferative activity (*12*).

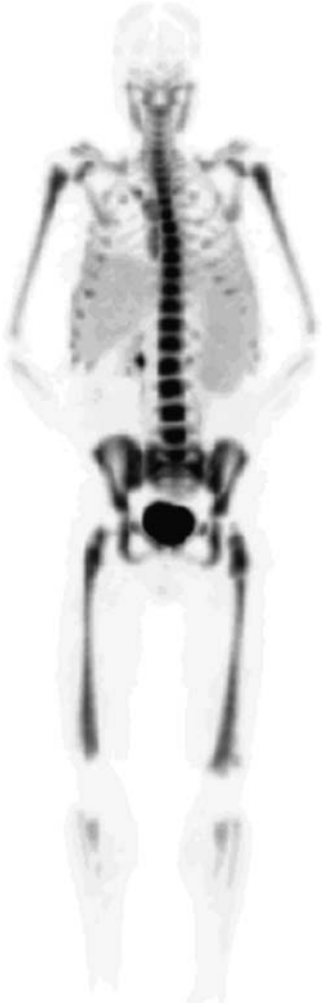

FIGURE 3. ^{18}F-FLT PET in patient with MDS shows homogeneously increased uptake and modest peripheral bone marrow expansion into peripheral bones.

FIGURE 4. ^{18}F-FLT PET in patient with myeloproliferative disorder shows homogeneously increased uptake and extensive peripheral bone marrow expansion into extremity bones.

Studies comparable to the present study have been performed in the past, using a multitude of tracers, such as iron isotopes for imaging and turnover studies of the erythropoietic precursor (*2–4*), ^{99m}Tc-labeled antigranulocyte antibodies for imaging of myeloid cells (*7–9*), radiocolloids for RES cell activity, and ^{111}In-choride. Compared with those methods, ^{18}F-FLT PET has a considerably higher resolution, produces tomographic information, and allows better quantification. Moreover, it might provide more specific information about the bone marrow compartment than a reflection of the functional activity of the RES.

CONCLUSION

^{18}F-FLT PET provides visual and quantitative information on the entire bone marrow compartment studied in a limited number of patients with hematologic disorders. This

FIGURE 5. ^{18}F-FLT PET in patient with myelofibrosis shows low uptake in bone marrow compartment, hepatosplenomegaly with increased uptake as result of extramedullary hematopoiesis, and minor bone marrow expansion into extremity bones.

may help in distinguishing various bone marrow disorders and be of value in the diagnostic follow-up of these patients.

ACKNOWLEDGMENTS

We thank Philip Elsinga, PhD, and his radiochemical staff for providing FLT.

REFERENCES

1. Palutke M, Tabaczka PM, Kukuruga DL, Kantor NL. A method for measuring lymphocyte proliferation in mixed lymphocyte cultures using a nuclear proliferation antigen, Ki-67, and flow cytometry. *Am J Clin Pathol.* 1989;91:417–421.
2. Kahn E, Aubert B, Parmentier C, Di Paola R. Feasibility of a ^{59}Fe ferrokinetic study based on bone-marrow scans. *Eur J Nucl Med.* 1983;8:312–316.
3. Ferrant A, Rodhain J, Leners N, et al. Quantitative assessment of erythropoiesis in bone marrow expansion areas using ^{52}Fe. *Br J Haematol.* 1986;62: 247–255.
4. Lubberink M, Tolmachev V, Beshara S, Lundqvist H. Quantification aspects of patient studies with ^{52}Fe in positron emission tomography. *Appl Radiat Isot.* 1999;51:707–715.
5. Horn NL, Bennett LR, Marciano D. Evaluation of aplastic anemia with indium chloride In 111 scanning. *Arch Intern Med.* 1980;40:1299–1303.
6. Pauwels EK, Hermans J, Jurgens PJ, Tjon Pian Gi CE, Haak HL, te Velde J. Scintigraphic aspects of ^{111}In-chloride bone marrow scintigraphy in aplastic anaemia. *Diagn Imaging.* 1981;50:269–276.
7. Jamar F, Field C, Leners N, Ferrant A. Scintigraphic evaluation of the haemopoietic bone marrow using a ^{99m}Tc-anti-granulocyte antibody: a validation study with ^{52}Fe. *Br J Haematol.* 1995;90:22-30.
8. Chung JK, Yeo J, Lee DS, et al. Bone marrow scintigraphy using technetium-99m-antigranulocyte antibody in hematologic disorders. *J Nucl Med.* 1996;37: 978–982.
9. Huic D, Ivancevic V, Richter WS, Munz DL. Immunoscintigraphy of the bone marrow: normal uptake values of technetium-99m-labeled monoclonal antigranulocyte antibodies. *J Nucl Med.* 1997;38:1755–1758.
10. Shields AF, Grierson JR, Dohmen BM, et al. Imaging proliferation in vivo with [F-18]FLT and positron emission tomography. *Nat Med.* 1998;4:1334–1336.
11. Been LB, Suurmeijer AJ, Cobben DC, Jager PL, Hoekstra HJ, Elsinga PH. [^{18}F]FLT-PET in oncology: current status and opportunities. *Eur J Nucl Med Mol Imaging.* 2004;31:1659–1672.
12. Brada SJ, van de Loosdrecht AA, Koudstaal J, de Wolf JT, Vellenga E. Limited numbers of apoptotic cells in fresh paraffin embedded bone marrow samples of patients with myelodysplastic syndrome. *Leuk Res.* 2004;28:921–925.
13. Grierson JR, Shields AF. Radiosynthesis of 3′-deoxy-3′-[^{18}F]fluorothymidine: [^{18}F]FLT for imaging of cellular profileration in vivo. *Nucl Med Biol.* 2000; 27:143–156.
14. Greenberg P, Cox C, LeBeau MM, et al. International scoring system for evaluating prognosis in myelodysplastic syndromes. *Blood.* 1997;89:2079–2088.
15. Been LB, Elsinga PH, de Vries J, et al. Positron emission tomography in patients with breast cancer using ^{18}F-3′-deoxy-3′-fluoro-l-thymidine (^{18}F-FLT): a pilot study. *Eur J Surg Oncol.* 2006;32:39–43.
16. van Westreenen HL, Cobben DC, Jager PL, et al. Comparison of ^{18}F-FLT PET and ^{18}F-FDG PET in esophageal cancer. *J Nucl Med.* 2005;46:400–404.
17. Cobben DC, Elsinga PH, Hoekstra HJ, et al. Is ^{18}F-3′-fluoro-3′-deoxy-L-thymidine useful for the staging and restaging of non-small cell lung cancer? *J Nucl Med.* 2004;45:1677–1682.
18. Cobben DC, Elsinga PH, Suurmeijer AJ, et al. Detection and grading of soft tissue sarcomas of the extremities with ^{18}F-3′-fluoro-3′-deoxy-L-thymidine. *Clin Cancer Res.* 2004;10:1685–1690.
19. Cobben DC, van der Laan BF, Maas B, et al. ^{18}F-FLT PET for visualization of laryngeal cancer: comparison with ^{18}F-FDG PET. *J Nucl Med.* 2004;45:226–231.
20. Cobben DC, Jager PL, Elsinga PH, Maas B, Suurmeijer AJ, Hoekstra HJ. 3′-^{18}F-Fluoro-3′-deoxy-L-thymidine: a new tracer for staging metastatic melanoma? *J Nucl Med.* 2003;44:1927–1932.
21. Span LF, Vierwinden G, Pennings AH, Boezeman JB, Raymakers RA, de Witte T. Programmed cell death is an intrinsic feature of MDS progenitors, predominantly found in the cluster-forming cells. *Exp Hematol.* 2005;33: 435–442.
22. Houwerzijl EJ, Blom NR, van der Want JJ, et al. Increased peripheral platelet destruction and caspase-3-independent programmed cell death of bone marrow megakaryocytes in myelodysplastic patients. *Blood.* 2005;105:3472–3479.
23. Barthel H, Perumal M, Latigo J, et al. The uptake of 3′-deoxy-3′-[^{18}F]fluorothymidine into L5178Y tumors in vivo is dependent on thymidine kinase 1 protein levels. *Eur J Nucl Med Mol Imaging.* 2005;32:257–263.
24. Van Waarde A, Cobben DC, Suurmeijer AJ, et al. Selectivity of ^{18}F-FLT and ^{18}F-FDG for differentiating tumor from inflammation in a rodent model. *J Nucl Med.* 2004;45:695–700.